Quantitative development of soil crack networks in clay and silty clay soils of Northern Iraq under repeated wetting – drying cycles using image analysis

Sulav Salim Sulaiman[1*] and Akram Abbas Khalaf [2*]

[1,2]Soil and Water Sciences Dept. College of Agricultural Engineering Science, university of Duhok, Kurdistan Region-Iraq

Corresponding author's email: Sulav Salim Sulaiman[1] ,solaf.sulaiman@uod.ac

Email addresses of coauthors: Akram Abbas Khalaf ,Akram.khalaf@uod.ac

Abstract

Soil cracking generated by repeated wetting–drying cycles strongly affects water movement, solute transport, and structural stability in clay-rich soils. Despite its importance, quantitative field-based evidence on the evolution of crack morphology under natural moisture cycles remains limited. This study investigated the development of surface crack characteristics in clay and silty clay soils from the Duhok region, northern Iraq, using a field-exposed wetting–drying experiment combined with image-based analysis. Five successive wetting–drying cycles were conducted under field conditions, and soil surface images were analyzed using ImageJ to quantify crack number, crack area, crack area percentage, mean crack width, total crack length, and connectivity index (CI).Mixed-effects modeling indicated that wetting–drying cycles significantly influenced all crack parameters ($p < 0.001$). Crack number and crack area were highest during the first cycle and decreased rapidly before stabilizing after the third cycle. In contrast, mean crack width and connectivity increased progressively with repeated cycles, indicating a transition from numerous fine cracks to fewer, wider, and more interconnected fractures. Soil texture had no significant effect on crack number, crack area, crack area percentage, or total crack length; however, clay soil exhibited significantly greater crack width and connectivity than silty clay.These findings demonstrate that repeated wetting–drying under field conditions promotes the maturation and stabilization of surface crack systems, with important implications for preferential flow and soil degradation processes in clay-dominated environments.

Key words: Soil crack networks, Wetting and drying cycles, Expansive soil, Image J analysis, crack connectivity index, mixed – effects model , field experiment

ISSN 2072-3857

Introduction

Soil cracking caused by successive wetting and drying cycles is a critical process in clay –dominated soils. It strongly influences their hydraulic, mechanical and environmental properties. Drying induces shrinkage, which produces tensile stresses that surpass the tensile strength of soil, resulting in surface fissures that serve as preferential flow pathways, diminish bearing capacity, and expedite erosion and solute transport [25,22, 23] In natural climatic settings, soils experience cycles of wetting and drying, leading to the development of fracture networks through the processes of initiation, propagation, coalescence, and stabilization, Rather than forming independently during each cycle [22, 26].Field studies have shown that soil fracture characteristics, such as crack number, crack length, crack area, and crack connectivity, experience dynamic alterations in response to natural rainfall and evaporation cycles. Rapid fracture initiation frequently occurs during the initial phases of drying, and successive cycles result in the expansion, branching, and interconnection of pre-existing cracks [24, 26]. The networks of surface fissures significantly influence hydrological processes at the landscape scale by enhancing preferential flow, increasing variability in infiltration, and altering the movement of water through the soil post-precipitation[14].The quantity and shape of cracks observed in the field are influenced by the soil's texture, clay content, and mineral composition, as well as the initial moisture content and climatic conditions, including precipitation, drying duration, and temperature. Clay soils generally have a greater propensity for shrinking and cracking compared to silty-clay soils due to their higher clay content and increased sensitivity to moisture fluctuations[15, 19].Repeated cycles of natural wetting and drying can weaken soil structure,increase surface roughness, And enhance susceptibility to erosion and degradation[11].Accurate measurement of soil cracks in the field is essential for comprehending soil's physical behavior and enhancing land and water management practices. Conventional field observations and manual measurements may be plagued by subjectivity and insufficient spatial resolution. In recent years, image processing techniques have increasingly been employed to analyze fractures in agricultural soil. This has enabled an objective and reproducible assessment of crack morphology. Image-based methodologies provide the direct quantification of crack area, length, width, density, connectivity, circularity, and solidity from field photographs [10,16].The ImageJ program is widely regarded as a premier instrument due to its cost-free accessibility and capability to do both particle-based and skeleton-based crack evaluations[20,21].In arid and semi-arid areas like Iraq and the Kurdistan Region, soils undergo significant seasonal variations between precipitation and drought, fostering circumstances conducive to recurrent wetting–drying cycles and the formation of surface cracks. Notwithstanding this, empirical investigations on soil fissuring in the region are still few. Research in Iraq has shown that natural wetting and drying substantially influence surface cracking and the structural behavior of fine-grained soils [1] .Recent research has emphasized that cyclical climatic conditions modify essential physical features of Iraqi soils, highlighting the necessity of examining soil cracking in actual field conditions [2].However, few studies have applied quantitative image analysis with statistical comparisons to evaluate soil crack characteristics under natural field conditions.. There remains a lack of comprehensive field-based investigations that quantitatively evaluate soil crack morphology and connectivity using image-processing approaches, particularly for

ISSN 2072-3857

clay and silty clay soils in the northern region of Iraq. Therefore, reliable and quantitative techniques are required to accurately characterize soil crack morphology and network development under natural field conditions**.** In this context, the present study investigates the formation and evolution of surface cracks in clay and silty clay soils from Duhok Province under repeated wetting–drying cycles in an open-field environment. ImageJ software was employed to quantitatively extract surface crack attributes and connectivity parameters from field-acquired images. The results aim to improve understanding of soil crack dynamics in relation to local climatic conditions and to provide scientific support for soil management and conservation strategies in semi-arid regions.

Objectives

The specific objectives of this investigation were:
1. Assess the variations in the number, area, percentage area, mean width, and total length of cracks across multiple wetting-drying cycles in clay and silty clay soils.
2. Analyze the Connectivity Index (CI) to quantify the evolution of crack interconnectedness over time and the transition from isolated cracks into well-connected fracture networks.
3. Statistically evaluate differences in crack morphology and network connectivity between clay and silty clay soils during successive wetting–drying cycles.

Material and methods
Study area and soil sampling

Soil samples were collected from representative sites in the Semel and Shekhan districts of the Duhok Governorate, Kurdistan Region, northern Iraq (Figure 1). At each site, soil was sampled from the 0–50 cm layer, which represents the active soil profile involved in moisture redistribution during wetting–drying cycles. Although surface cracks primarily manifest in the upper soil layer, the deeper soil contributes to crack initiation and evolution by supplying water, controlling shrink–swell behavior, and influencing stress redistribution during drying.

Soil collected from multiple points within each site was thoroughly mixed to form a composite sample representative of local soil conditions. The samples were air-dried, gently crushed, and sieved through a 4-mm mesh prior to laboratory characterization and experimental use.

Physical properties of both sites

Basic physical properties were determined to characterize and classify the studied soils. These measurements were conducted on composite samples and were not subjected to statistical comparison.Soil physical properties were assessed using standard ASTM and internationally recognized methods, encompassing particle-size distribution (ASTM D7928-17)[9], Atterberg limits (ASTM D4318) [8] ,bulk density (ASTM D7263)[6], particle density (ASTM D854) [4],moisture content (ASTM D2216)[7], Proctor compaction (ASTM D698) [3], field capacity, and permanent wilting point

via pressure-plate apparatus (ASTM D6836) [5], (Table 1).

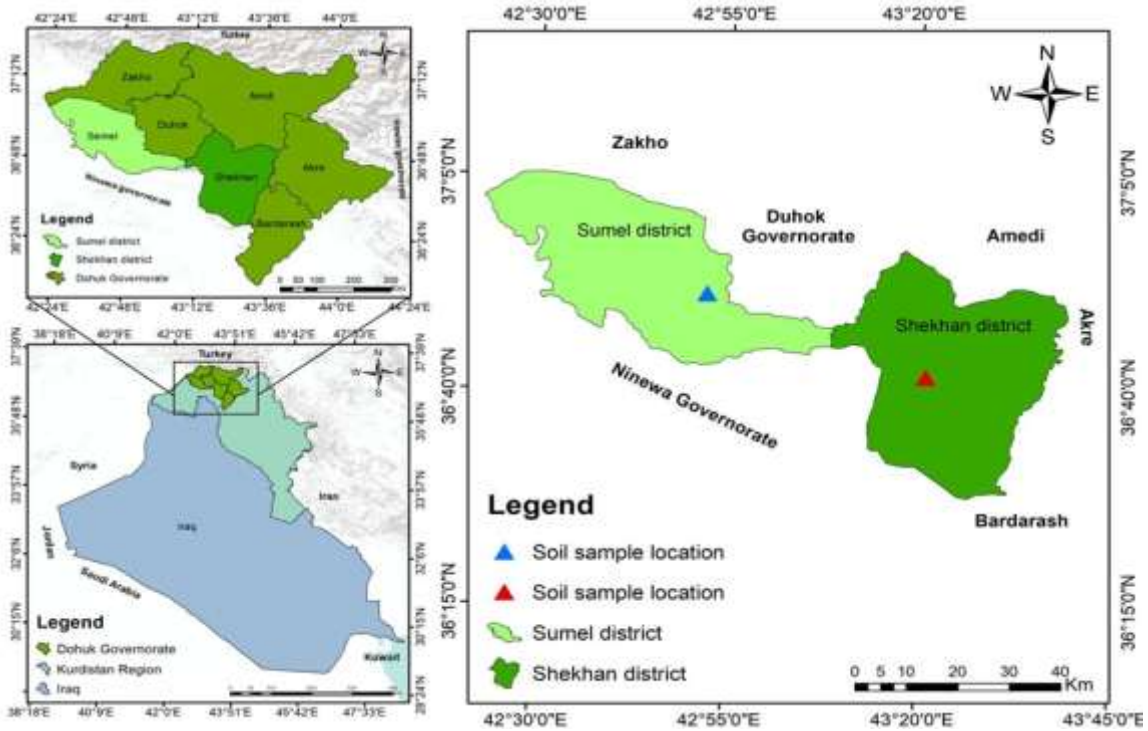

Figure 1: Location of soil sampling sites in Semel and Shekhan districts, Duhok Governorate, Kurdistan Region, Iraq.

Table 1: Basic physical properties of both sites.

Soil properties	unit	Shekhan	Semel
Specific gravity		2.71	2.63
Bulk density	g cm^{-3}	1.46	1.39
Initial moisture	%	4.82	4.12
Optimum moisture	%	23.35	18.75
Particle size distribution			
Sand	%	6.2	7.4
Silt	%	33.6	40
clay	%	60.2	52.6
Textural type		clay	silty clay
Atterberg limits			
Liquid limit	%	48.80	46.08

ISSN 2072-3857

Plastic limit	%	33.74	32.14
Plastic index	%	15.06	13.94
Field capacity	%	38.05	33.66
Wilting point	%	29.23	24.13

Experimental location

The wetting–drying cycle experiment was conducted under open-field conditions at the University of Duhok, College of Agriculture, located in the Duhok Governorate, Kurdistan Region, northern Iraq. The experimental site is situated at 36°51′27.57″ N latitude and 42°52′08.08″ E longitude, at an elevation of approximately 475 m above sea level. The region is characterized by a semi-arid Mediterranean climate, with hot, dry summers and cool, wet winters. Mean annual rainfall is concentrated mainly between November and March, while prolonged dry periods with high evaporative demand typically occur during late spring and summer. These climatic conditions promote repeated natural wetting–drying cycles, making the site well suited for investigating soil cracking behavior under field conditions. The experimental setup was fully exposed to natural atmospheric factors, including air temperature, wind, relative humidity, and evaporation.

Experimental design

Following collection from the Semel and Shekhan sites, the soils were air-dried, carefully crushed, and sieved through a 4-mm mesh prior to pot preparation. Two soil types were used: clay soil and silty clay soil. Three replicate pots were prepared for each soil type, resulting in a total of six experimental units. Cylindrical metal pots with an internal diameter of 30 cm and a height of 30 cm were used. Each pot was filled with soil to a height of 26 cm, leaving approximately 4 cm of free space at the top to allow water application during saturation without overflow. The pots were non-perforated at the bottom, ensuring that no drainage occurred during wetting and drying. This design was adopted to maintain controlled moisture redistribution within the soil profile and to simulate field conditions where surface cracking develops primarily under evaporation-driven drying rather than gravitational drainage.The clay soil was adjusted to its optimum moisture content (23.35%) and compacted to a bulk density of 1.46 g cm^{-3}, while the silty clay soil was conditioned to an optimum moisture content of 18.75% and a bulk density of 1.39 g cm^{-3}. The required amount of water was calculated based on oven-dry soil mass and target moisture content. Water was added gradually and mixed thoroughly, after which the soils were covered and allowed to equilibrate for 24 h to ensure uniform moisture distribution. The moist soils were placed in layers and lightly compacted to achieve the target bulk densities. The six pots were then positioned in an open experimental area at the University of Duhok, College of Agriculture, where the soil surface was fully exposed to natural atmospheric conditions, including solar radiation, air temperature, wind, and evaporation.

Wetting–drying cycle procedure and environmental monitoring

After soil preparation, the wetting-drying experiment was started. During each cycle, water was carefully added to the soil surface of each pot until saturation was reached, as evidenced by the presence of free water on the soil. The pots were then

ISSN 2072-3857

allowed to dry naturally in open-field conditions until soil moisture reached the wilting point or the surface crack pattern became visually stable, marking the end of the drying process. This method was repeated five times. The length of each cycle varied according on meteorological conditions and evaporation demands. The start and end dates of each cycle were recorded, as well as the average meteorological conditions during each wetting-drying cycle, in order to identify the environmental drivers of soil drying and crack development (Table 2). The variables monitored were air temperature, wind speed, relative humidity, and pan evaporation. These characteristics have been shown to control soil water loss and crack evolution in the field [12]. Climatic data, including air temperature, wind speed, relative humidity, and evaporation, were collected from the Duhok Meteorological Station, which is run by the Iraqi Meteorological and Seismology Organization [13].

Table 2: Duration of wetting–drying cycles and corresponding climatic conditions recorded at the Duhok Meteorological Station.

Cycle	Start date	End date	Air temperature (°C) Min	Air temperature (°C) Max	Wind speed (m s^{-1})	Relative humidity (%) Min	Relative humidity (%) Max	Evaporation (mm day^{-1})
1	22/09/2024	30/09/2024	20	34.1	1.19	24	58.6	5.83
2	30/09/2024	8/10/2024	18.2	33	1	21	54.9	4.75
3	8/10/2024	13/10/2024	19.7	34.7	0.95	17	45.3	5.07
4	13/10/2024	23/10/2024	15.1	27.4	1.18	22	56.9	3.65
5	23/10/2024	7/11/2024	10.52	23.34	1.05	30	65.7	2.3

Note: Climatic data were obtained from the Duhok Meteorological Station operated by the Iraqi Meteorological and Seismology Organization.

Image processing and crack quantification

Digital photographs of soil surface cracks were captured at the end of each drying stage for all wetting–drying cycles and analyzed using ImageJ (Fiji distribution). Images were acquired using an iPhone 15 camera with a high-resolution sensor, positioned vertically at a fixed height of approximately 50 cm above the soil surface to ensure consistent spatial resolution across all images. Photography was conducted under uniform natural daylight conditions, avoiding shadows and extreme illumination variations to minimize lighting-induced artifacts. The image-processing workflow followed the standardized procedure illustrated in Figure 2. The original RGB images were cropped to the circular soil surface using a region of interest (ROI) corresponding to the fixed internal diameter of the pot. All images were spatially calibrated in ImageJ using this fixed pot diameter as a reference scale, ensuring that pixel-based measurements were converted into real-world units (cm) independently of

soil surface shrinkage occurring during successive wetting–drying cycles.

The images were then converted to 8-bit grayscale, and noise and uneven illumination were reduced using median filtering and background subtraction. An appropriate threshold was applied to separate cracks from the soil matrix, producing binary images in which cracks were represented as foreground pixels. A binary opening operation was applied to remove isolated noise while preserving true fracture features. Crack area, crack number, and crack area percentage were quantified from binary images using the Analyze Particles tool, with crack area percentage calculated as the ratio of total crack area to total soil surface area within the ROI. Crack width was calculated using the distance map generated from the binary images, where each crack pixel was assigned the shortest distance to the nearest crack boundary and local crack width was estimated as twice that distance. Mean crack width was obtained by averaging the spatially calibrated local width values across the entire crack network. To quantify crack length and connectivity, the binary images were skeletonized to generate one-pixel-wide representations of the crack network. Skeletonized images were analyzed using the Analyze Skeleton (2D/3D) plugin to extract total crack length, number of branches, and number of junctions, which describe the geometric complexity and connectivity of the crack network. Crack network connectivity was quantified using the connectivity index (CI), following the approach proposed by Shit et al. (2015). The CI describes the topological interconnection of the crack network and was calculated from skeletonized crack images as:

$$CI = L / L\,max = L / [3(V - 2)]$$

where L represents the number of connected crack links and V represents the number of crack junctions (nodes). CI values range from 0 to 1, with higher values indicating a more interconnected and continuous crack network.This image-based approach provides objective and reproducible quantification of soil crack geometry and topology and has been widely applied in soil cracking studies [17,20,22]. Figure 3 illustrates representative steps of the image-processing procedure.

Statistical analysis

connectivity index) were analyzed using linear mixed-effects models to evaluate the effects of soil type, wetting–drying cycle, and their interaction. Soil type and cycle were treated as fixed effects, while replication nested within soil type was included as a random effect. Variance components were estimated using restricted maximum likelihood (REML) with Kenward–Roger degrees of freedom. When significant effects were detected, Tukey's HSD test was applied for post hoc multiple comparisons. Results are presented as mean ± SD, and model assumptions were verified using residual diagnostics. All statistical tests were two-tailed, and significance was assessed at a probability level of $\alpha = 0.05$. Statistical analyses were performed using Minitab 19.

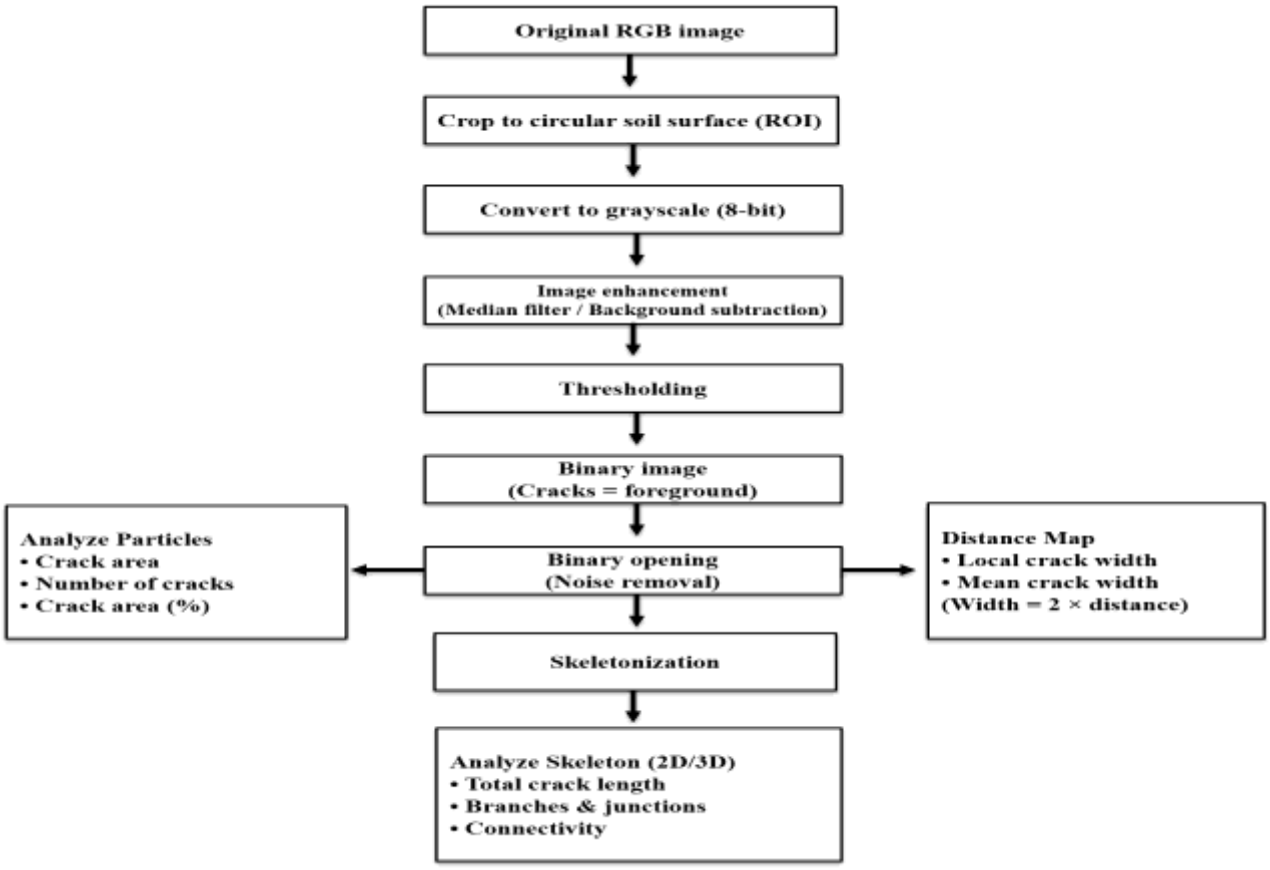

Figure 2: ImageJ-based workflow for soil crack image processing and analysis

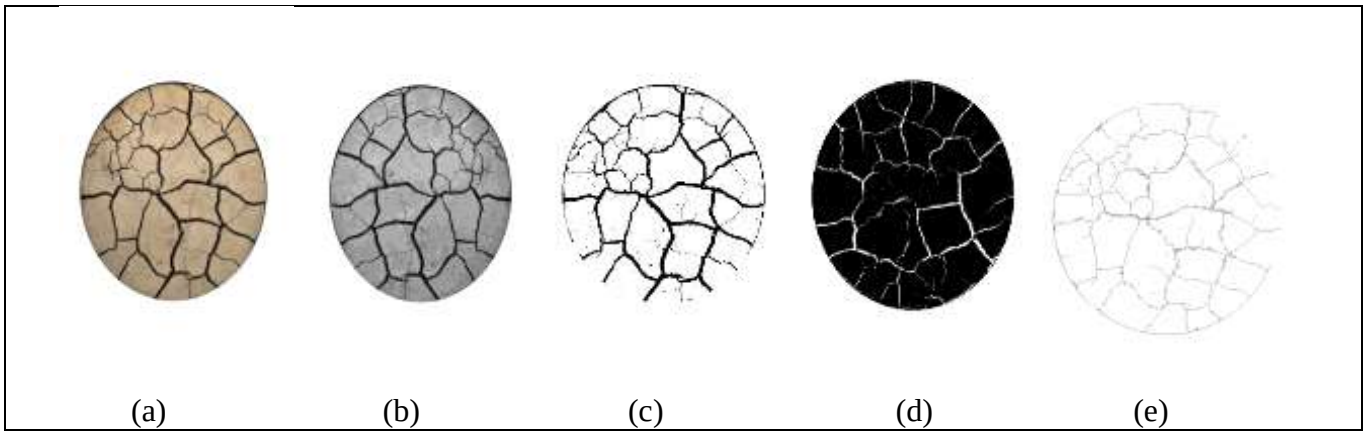

Figure 3: Crack image processing process: (a) original image; (b) grayscale image; (c) binary image; (d) distance map image; (e) skeletonized image.

Results and Discussion

Visual progression of soil cracking during wetting and drying cycles

Figures 4 and 5 show binary pictures of soil surface cracks in clay and silty-clay soils across five wetting-drying cycles. Each figure represents three independent replications each cycle.

Quantitative crack parameters

The visual discrepancies between Figures 4 and 5were validated by a quantitative study of ImageJ crack metrics such as crack

ISSN 2072-3857

number, crack area percentage, total crack area, mean crack width, total crack length, and connectivity index. These values were computed for each replication and then averaged across soil types and cycles (Table3).

Impact of weather conditions on fracture formation

The variation in crack development across wetting–drying cycles was strongly influenced by atmospheric drying demand, as reflected by air temperature, relative humidity, and evaporation rate (Table 2). For example, Cycle 3, which exhibited the highest maximum air temperature (34.7 °C), the lowest minimum relative humidity (17%), and a high evaporation rate (5.07 mm day^{-1}), showed the most rapid soil drying and earlier stabilization of surface cracks. In contrast, Cycle 5, characterized by lower temperatures, higher relative humidity, and the lowest evaporation rate (2.3 mm day^{-1}), experienced slower drying and more gradual crack development. These quantitative differences indicate that higher evaporative demand accelerates soil moisture loss, promotes faster shrinkage, and enhances crack initiation and propagation. This observation is consistent with soil physics principles, which recognize evaporation rate as a primary driver of soil desiccation and crack evolution under field conditions [12].

Table 3: Quantitative crack characteristics of clay and silty-clay soils obtained from image J analysis.

Cycle	Soil Type	R	Crack Number	Crack Area cm^2	Crack Area %	Mean Width (cm)	Total Length (cm)	Connectivity Index (CI)
1	Clay	1	89	29.901	4.968	0.47	251.85	0.2
		2	49	27.214	4.863	0.57	289.97	0.22
		3	43	19.856	3.686	0.45	219.58	0.21
	Silty Clay	1	66	22.603	4.345	0.37	233.362	0.19
		2	73	22.82	3.899	0.3	223.245	0.19
		3	68	19.87	3.365	0.25	236.113	0.2
2	Clay	1	41	11.114	2.162	0.67	277.737	0.21
		2	29	8.765	1.696	0.66	295.516	0.23
		3	50	15.075	2.75	0.64	238.398	0.22
	Silty Clay	1	33	12.9	2.155	0.63	289.042	0.21
		2	44	11.356	2.159	0.48	260.441	0.2
		3	37	12.976	2.431	0.6	261.765	0.22
3	Clay	1	16	7.103	1.207	1.08	309.19	0.23

ISSN 2072-3857

		2	18	5.821	1.016	1.06	302.658	0.23
		3	18	5.388	1.068	1.04	284.061	0.23
	Silty Clay	1	22	6.037	1.156	0.71	300.75	0.21
		2	23	7.016	1.167	0.74	279.141	0.2
		3	29	6.412	1.145	0.72	260.289	0.21
4	**Clay**	1	16	5.557	0.973	0.98	289.826	0.24
		2	14	4.836	0.916	1.05	292.598	0.23
		3	16	5.231	1.029	1.05	261.349	0.23
	Silty Clay	1	15	6.023	1.114	0.64	285.425	0.21
		2	23	5.498	1.02	0.76	257.224	0.2
		3	22	5.176	1.124	0.89	236.783	0.22
5	**Clay**	1	15	5.197	0.981	0.91	267.098	0.24
		2	12	4.753	0.991	1.16	253.572	0.24
		3	14	5.129	1.039	1.12	251.205	0.22
	Silty Clay	1	16	6.101	1.179	0.799	261.948	0.22
		2	20	4.859	0.964	0.73	238.42	0.22
		3	24	5.153	1.074	0.69	235.58	0.22

ISSN 2072-3857

Cycles	R1	R2	R3
First cycle	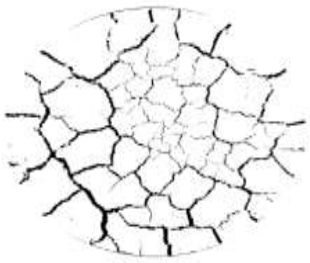		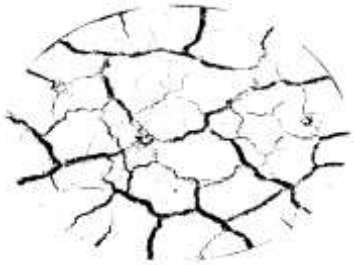
Second cycle	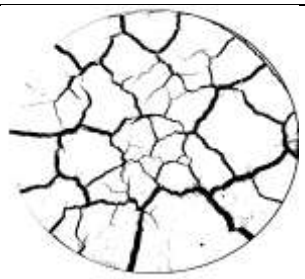		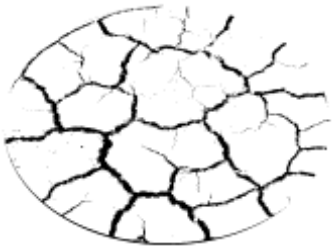
Third cycle	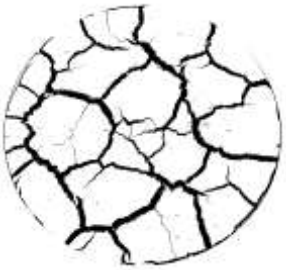	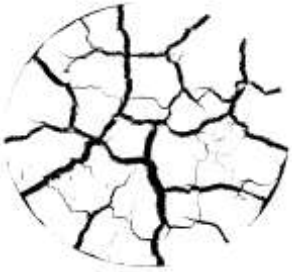	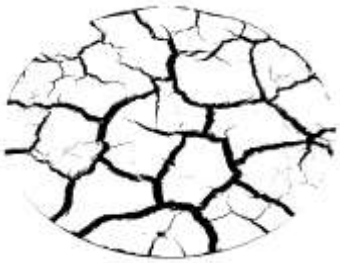
Fourth cycle		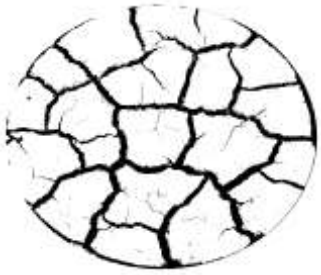	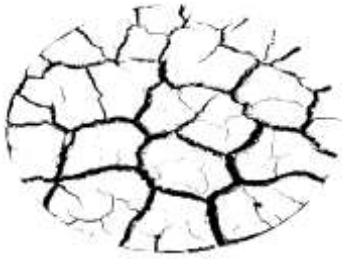
Fifth cycle		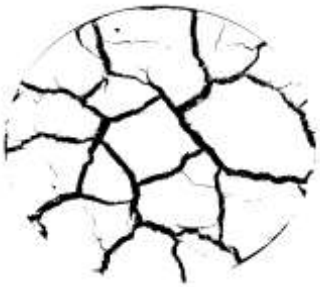	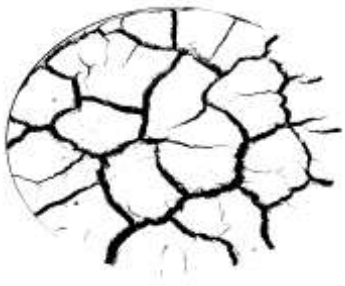

Figure 4: Binary crack images of clay soil during five wetting–drying cycles (three replications per cycle).

ISSN 2072-3857

Cycles	R1	R2	R3
First cycle		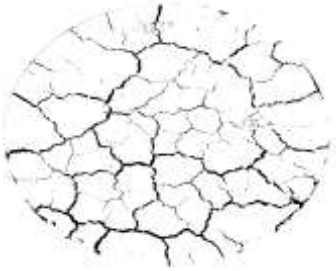	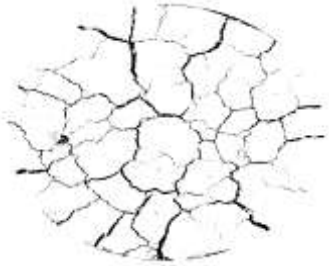
Second cycle		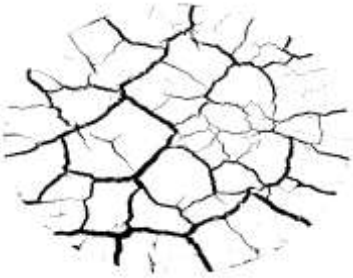	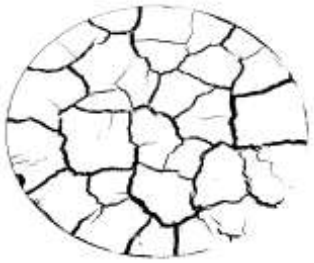
Third cycle		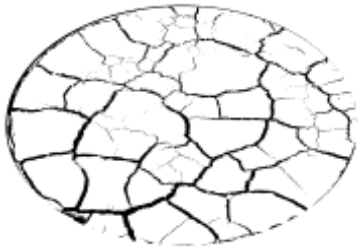	
Fourth cycle	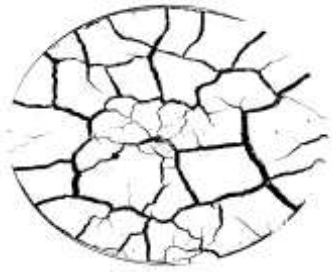	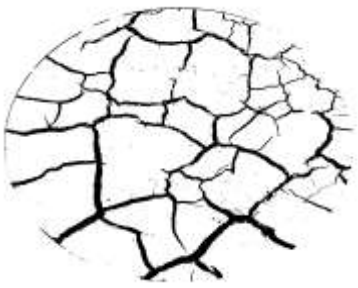	
Fifth cycle	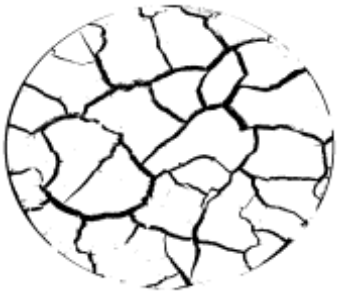		

Figure 5: Binary crack images of silty clay soil during five wetting–drying cycles (three replications per cycle).

ISSN 2072-3857

Effect of wetting–drying cycles on crack number

The mixed-effects model showed that wetting–drying cycles had a highly significant effect on crack number ($P < 0.001$), whereas soil type ($P = 0.257$) and the soil type × cycle interaction ($P = 0.849$) were not significant (Table 4). This indicates that crack frequency was primarily controlled by the temporal progression of wetting–drying cycles rather than by soil texture. As illustrated in Figure 6 and Table 5, crack number in both clay and silty clay soils was highest during the first wetting–drying cycle and decreased markedly with successive cycles, reaching relatively stable values by the fourth and fifth cycles. The pooled Tukey comparison across cycles (Table 6) confirmed that cycle 1 formed a distinct high-crack group, cycle 2 represented an intermediate group, while cycles 3–5 were statistically similar and characterized by low crack numbers. The significant reduction in crack number with successive wetting–drying cycles reflects a progressive reorganization of the soil fracture system driven by cyclic shrink–swell processes. During the initial drying cycle, rapid moisture loss induces high tensile stresses, leading to the formation of numerous fine and discontinuous cracks. With repeated wetting and drying, these initial cracks propagate and coalesce, resulting in fewer but more continuous fracture pathways. This mechanism has been widely reported in cracking-prone soils, where early drying stages are characterized by high crack density followed by a consolidation and stabilization of the crack network in later cycles [22].The lack of a significant soil type effect on crack number further suggests that crack initiation and subsequent reorganization are primarily controlled by moisture cycling rather than by moderate differences in soil texture between clay and silty clay. Similar behavior was observed by [23], who reported that silty clay soils subjected to repeated wetting–drying cycles exhibited a marked decrease in crack number as micro-cracks merged into larger fractures and soil aggregates rearranged. Together, these findings confirm that the evolution of crack number is governed by cyclic moisture dynamics and fracture coalescence rather than soil texture alone.

Table 4: Statistical significance of soil type, wetting–drying cycle, and their interaction on soil crack number

Term	P-Value	Interpretation
Soil Type	0.257	Not significant
Cycle	0.000	Highly significant
Soil Type*Cycle	0.849	Not significant

*Not significant ($P > 0.05$) and highly significant ($P < 0.001$).

Table 5: Descriptive statistics (mean ± standard deviation) of crack number for clay and silty clay soils under successive wetting–drying cycles.

Cycle	clay soil	silty clay soil
1	60.3 ± 25.0 ab	69.00±3.61 a
2	40.00 ± 10.54 bc	38.00±5.57 bcd
3	17.33 ± 1.16 cd	24.67±3.79 cd
4	15.33 ± 1.16 cd	20.00±4.36 cd
5	13.67 ± 1.52 d	20.00±4.00 cd

*Means that do not share a letter are significantly different ($P < 0.05$).

ISSN 2072-3857

Table 6: Tukey grouping of mean crack number across wetting–drying cycles (averaged over clay and silty clay soils).

Cycle	N	Mean
1	6	64.67 a
2	6	39.00 b
3	6	21.00 c
4	6	17.67 c
5	6	16.83 c

*Means that do not share a letter are significantly different ($P < 0.05$).

Effect of wetting–drying cycles on soil crack area

The mixed-effects model indicated that wetting–drying cycles had a highly significant effect on soil crack area ($P < 0.001$), whereas soil type ($P = 0.593$) and the soil type × cycle interaction ($P = 0.288$) were not significant (Table 7). This demonstrates that changes in crack area were primarily governed by moisture cycling rather than by differences between clay and silty clay soils. As shown in Figure 7 and Table8, crack area in both soils was greatest during the first wetting–drying cycle and declined sharply with subsequent cycles, reaching relatively stable values after the third cycle. Tukey's multiple comparison test (Table 9) separated the cycles into three statistically distinct groups, with the first cycle exhibiting the largest crack area, the second cycle showing an intermediate response, and cycles three to five forming a low and statistically similar group. The pronounced decrease in soil crack area with successive wetting–drying cycles indicates a progressive consolidation of the fracture system driven by cyclic shrink–swell processes. During the first drying cycle, rapid moisture loss induces high tensile stresses that promote the formation of extensive fracture surfaces, resulting in a large exposed crack area. As wetting–drying cycles continue, the generation of new fracture surfaces becomes limited, and structural rearrangement dominates, leading to a marked reduction and eventual stabilization of crack area.

This behavior is consistent with the findings of [1], who reported that desiccation crack area is highest during the initial drying stage and decreases as fractures consolidate and soil structure evolves. Similarly, [18] demonstrated that repeated wetting–drying cycles reduce exposed crack area by densifying the soil matrix and replacing dense networks of fine cracks with fewer, wider fractures. These studies support the interpretation that early wetting–drying cycles are primarily responsible for fracture surface development, whereas later cycles mainly promote crack merging and structural stabilization rather than further increases in surface exposure. The lack of a significant soil type effect on crack area suggests that, in fine-textured soils, moisture cycling exerts a stronger control on fracture surface evolution than moderate differences in texture. This observation agrees with [2], who showed that cyclic wetting–drying can outweigh textural contrasts in controlling fracture geometry in clay-dominated soils. Comparable trends were also reported by [23], where repeated wetting–drying cycles led to a rapid decline in crack area followed by stabilization as fracture networks matured and aggregate packing improved. Overall, these findings confirm that crack area evolution is governed primarily by the intensity and repetition of wetting–drying cycles, while soil texture plays a secondary role in fine-grained soils subjected to cyclic moisture stress.

ISSN 2072-3857

Table 7: Statistical significance of soil type, wetting–drying cycle, and their interaction on soil crack area

Term	P-Value	Interpretation
Soil Type	0.593	Not significant
Cycle	0.000	Highly significant
Soil Type*Cycle	0.288	Not significant

*Not significant (P > 0.05) and highly significant (P < 0.001).

Table 8: Descriptive statistics (mean ± standard deviation) of crack area for clay and silty clay soils under successive wetting–drying cycles.

Cycle	clay soil	silty clay soil
1	25.66 ± 5.20 a	21.76 ± 1.64 a
2	11.65 ± 3.19 bc	12.41 ± 0.91 b
3	6.10 ± 0.89 cd	6.49 ± 0.49 bcd
4	5.21 ± 0.36 d	5.57 ± 0.43 d
5	5.03 ± 0.24 d	5.37 ± 0.65 d

*Means that do not share a letter are significantly different (P < 0.05).

Table 9: Tukey grouping of mean crack area across wetting–drying cycles (averaged over clay and silty clay soils).

Cycle	N	Mean
1	6	23.71 a
2	6	12.03 b
3	6	6.30 c
4	6	5.39 c
5	6	5.20 c

*Means that do not share a letter are significantly different (P < 0.05).

Effect of wetting–drying cycles on soil crack area (%)

The mixed-effects model revealed that the wetting-drying cycle significantly impacted percentage crack area (P < 0.001), whereas soil type had no significant influence (P = 0.567) and the Soil Type × Cycle interaction was similarly not significant (P = 0.270). This suggests that the time evolution of surface cracking was predominantly influenced by repeated soaking and drying rather than soil texture.

Although there were slight numerical changes in percentage crack area between clay and silty clay in individual cycles (Figure 8), they were not statistically significant. Both soils demonstrated essentially comparable temporal trends, with high crack ratios in the first cycle and stable low values after the third cycle. This shows that crack area evolution was mostly regulated by moisture-induced shrink-swell behavior rather than mild changes in texture, comparable with earlier research on fine-grained soils [23,26].

The Tukey multiple comparison test (Table 12) determined that cycle 1 in group A had the highest percentage crack area, followed by cycle 2 in group B and cycles 3-5 in group C, all of which had significantly smaller crack areas. This suggests that the majority of surface cracking occurred during the initial drying step, but subsequent wetting-drying cycles restructured and stabilized the fracture network rather than forming new cracks. Recent experimental and theoretical

research on fine-grained soil desiccation cracking confirms this statistical trend. [26]discovered that expansive soils open fractures and expose the surface during the first wet-dry cycle before consolidating and stabilizing during subsequent cycles, hence reducing crack area. [25] discovered that clayey soils generate the majority of their crack area ratio during the initial drying stage, but subsequent wetting-drying cycles alter existing cracks rather than create new surface fractures.[2]shown that repeated wetting-drying and physical weathering alter soil structure and partially seal or merge micro-cracks, hence reducing total crack area.

The mean % crack area (±SD) for each soil and cycle is shown in Table 11. Clay and silty clay showed the highest crack area in the first wetting-drying cycle (4.51 ± 0.71% in clay and 3.87 ± 0.49% in silty clay), followed by a considerable decrease in the second cycle. From cycle 3, the crack area stabilized at 1.0-1.2% for cycles 3-5. Progressive crack network reorganization is shown here. Tensile strains generate several open fractures during the first drying, creating a broad crack surface. The total exposed crack surface decreases when cracks merge, widen, and rearrange into smaller, more stable fractures during wetting and drying. In clayey soils under shrink-swell processes, crack-area stabilization after early cycles is common [22,23,26].

Table 10: Statistical significance of soil type, wetting–drying cycle, and their interaction on soil crack area (%).

Term	P-Value	Interpretation
Soil Type	0.567	Not significant
Cycle	0.000	Highly significant
Soil Type*Cycle	0.270	Not significant

*Not significant (P > 0.05) and highly significant (P < 0.001).

Table 11: Descriptive statistics (mean ± standard deviation) of crack area (%) for clay and silty clay soils under successive wetting–drying cycles.

Cycle	clay soil	silty clay soil
1	4.51 ± 0.71 a	3.87 ± 0.49 a
2	2.20 ± 0.53 b	2.25 ± 0.16 b
3	1.10 ± 0.10 c	1.16 ± 0.01 c
4	0.97 ± 0.06 c	1.09 ± 0.06 c
5	1.00 ± 0.03 c	1.07 ± 0.11 c

*Means that do not share a letter are significantly different (P < 0.05).

Table 12: Tukey grouping of mean crack area (%) across wetting–drying cycles (averaged over clay and silty clay soils).

Cycle	N	Mean
1	6	4.19 a
2	6	2.23 b
3	6	1.13 c
4	6	1.03 c
5	6	1.04 c

*Means that do not share a letter are significantly different (P < 0.05).

ISSN 2072-3857

Effect of wetting–drying cycles on soil Mean crack width

The mixed-effects model revealed that soil type, wetting-drying cycle, and their interaction had a significant effect on mean crack width ($p < 0.001$ for soil type and cycle; $p = 0.042$ for the interaction). This shows that fracture width was influenced by both soil texture and repetitive wetting-drying, and that clay and silty clay didn't widen at the same rate.

Clay consistently had bigger fissures than silty clay (Figure 9). This difference grew more obvious in subsequent cycles, showing that clay soil's higher clay content and shrink-swell capacity resulted in increased tensile strains and crack opening. This behavior is consistent with the results of [18],who discovered that soils with higher clay content develop wider surface fractures after repeated wetting-drying due to increased volumetric shrinkage and stress concentration along crack walls. Similarly, [23]found that silty clay, despite forming cracks, has smaller crack openings than clay-rich soils due to less shrinkage potential.

Tukey's multiple comparison test (Table 15) showed wetting and drying cycles had different mean crack widths. Group A (cycles 3, 4, and 5) had the biggest statistical mean crack widths (0.90-0.91 cm), showing repeated wetting-drying increases cracks. Cycle 2 was intermediate (Group B) while Cycle 1 was lowest (Group C) with 0.402 cm crack width. This rating shows that wetting and drying deepen fissures. A large increase from Cycle 1 to Cycle 3 shows the evolution from microcracks to a fracture system. By Cycles 3-5, the fracture network had stabilized and could not expand. Early shrinkage cracks have small apertures due to fracture initiation, while subsequent cycles have larger apertures due to repeated shrinkage strain. Tu, Kamran, and Shaker found that crack widening accelerates early in cycles before plateauing as the fracture network grows.

Both soils' mean fracture width rose steadily over wetting-drying cycles (Figure 9; Table 14). Clay crack width rose from 0.50 ± 0.06 cm in cycle 1 to 1.06 ± 0.13 cm in cycle 5, while silty clay increased from 0.31 ± 0.06 cm to 0.74 ± 0.06 cm. During cyclic shrink-swell, the crack network widens. As tensile tensions mount, many fine cracks form during drying. These cracks reopen, propagate, and merge with repeated wetting-drying, creating fewer but larger, hydraulically active fractures. [23,19]associated micro-crack coalescence and soil structure rearrangement with crack-widening in clayey and silty clay soils under cyclic drying.

Table 13: Statistical significance of soil type, wetting–drying cycle, and their interaction on soil crack area

Term	P-Value	Interpretation
Soil Type	0.000	Highly significant
Cycle	0.000	Highly significant
Soil Type*Cycle	0.042	Significant

*Significant ($P < 0.05$) and highly significant ($p < 0.001$).

ISSN 2072-3857

Table 14: Descriptive statistics (mean ± standard deviation) of mean crack width for clay and silty clay soils under successive wetting–drying cycles.

Cycle	clay soil	silty clay soil
1	0.50 ± 0.06 cd	0.31 ± 0.06 d
2	0.66 ± 0.02 bc	0.57 ± 0.08 bc
3	1.06 ± 0.02 a	0.72 ± 0.02 b
4	1.03 ± 0.04 a	0.76 ± 0.13 b
5	1.06 ± 0.13 a	0.74 ± 0.06 b

*Means that do not share a letter are significantly different (P < 0.05).

Table 15: Tukey grouping of mean crack width across wetting–drying cycles (averaged over clay and silty clay soils).

Cycle	N	Mean
1	6	0.40 c
2	6	0.61 b
3	6	0.89 a
4	6	0.90 a
5	6	0.90 a

*Means that do not share a letter are significantly different (P < 0.05).

Effect of wetting–drying cycles on soil total crack length

The mixed-effects model found that the wetting-drying cycle significantly impacted total fracture length ($p < 0.001$), but soil type ($p = 0.340$) and the Soil Type × Cycle interaction ($p = 0.533$) were not significant. This demonstrates that the temporal evolution of cracking dominated the development of total fracture length, and that clay and silty clay had similar crack-length trends after repeated wetting-drying cycles. This is consistent with prior research, which found that crack length in fine-grained soils reacts mostly to moisture-driven shrink-swell processes rather to mild textural changes [21,22,26].

The mean total crack length (Figure 10) grew significantly from the first to the third wetting-drying cycle, then decreased marginally in subsequent cycles. In clay soil, total crack length increased from 253.8 cm in Cycle 1 to a peak of 298.6 cm in Cycle 3, then decreased to 281.3 cm in Cycle 4 and 257.3 cm in Cycle 5. A similar pattern was found in silty clay, where fracture length rose from 230.9 cm in Cycle 1 to 280.1 cm in Cycle 3, before gradually decreasing in Cycles 4 and 5.

Tukey's test (table 17) corroborated this tendency, with Cycle 3 ranked highest (A), Cycles 2 and 4 intermediate (A-B), and Cycle 1 lowest (C). This suggests that crack networks attained their maximal expansion after a few wetting-drying cycles before stabilizing. This pattern shows the structural evolution of the soil crack network. Cracks are short and discontinuous during the first drying cycle, but as more cycles are performed, cracks propagate, connect together, and extend, resulting in longer continuous fractures. [22]shown that repeated wetting-drying causes progressive crack propagation and coalescence, increasing overall crack length even when the number of cracks decrease. [21]found that the total crack length is a sensitive measure of crack network development, including fracture growth and linking. [26]discovered that crack length increases when micro-cracks

combine into dominant fractures, following which continued cycling primarily stabilizes the network.

Clay had a slightly larger mean total crack length (272.3 cm) than silty clay (257.3 cm), but the mixed-effects model (p = 0.340) and Tukey test showed no statistically significant difference (Table 18). It appears that soil type did not affect crack network extension. Instead, fine-textured, shrink-swell-dominated soils share a similar characteristic in which moisture-induced volume change and suction control crack formation rather than moderate silt content fluctuations. [26]discovered that fine-grained soils with high clay activity had similar crack-length evolution during wetting-drying, while [22]found that drying stress and aggregate rearrangement affect crack propagation more than particle-size variation.

Table 16: Statistical significance of soil type, wetting–drying cycle, and their interaction on soil total crack length.

Term	P-Value	Interpretation
Soil Type	0.340	Not significant
Cycle	0.000	Highly significant
Soil Type*Cycle	0.533	Not significant

*Not significant (P > 0.05) and highly significant (P < 0.001).

Table 17: Tukey grouping of mean total crack length across wetting–drying cycles (averaged over clay and silty clay soils).

Cycle	N	Mean
1	6	242.35 c
2	6	270.48 ab
3	6	289.35 a
4	6	270.53 ab
5	6	251.30 bc

*Means that do not share a letter are significantly different (P < 0.05).

Table 18: Descriptive statistics (mean ± standard deviation) of mean total crack length for clay and silty clay soils under successive wetting–drying cycles.

Cycle	clay soil	silty clay soil
1	253.8 ± 35.2 bc	230.91 ± 6.78 c
2	270.6 ± 29.2 abc	270.42 ± 16.14 ab
3	298.64 ± 13.04 a	280.1 ± 20.2 ab
4	281.26 ± 17.30 abc	259.8 ± 24.4 abc
5	257.29 ± 8.57 bc	245.32 ± 14.47abc

*Means that do not share a letter are significantly different (P < 0.05).

ISSN 2072-3857

Effect of wetting–drying cycles on soil connectivity index (CI)

The mixed-effects model revealed that soil type ($p = 0.015$) and wetting-drying cycle ($p < 0.001$) had significant effects on connectivity index. However, the interaction between soil type and cycle was not significant ($p = 0.363$). This suggests that both soils formed increasingly connected fracture networks during subsequent wetting-drying cycles, although the temporal pattern of connectivity growth was same in clay and silty clay.

Figure 11 displays the mean Connectivity Index for clay and silty clay over five wetting-drying cycles. In both soils, CI increased with subsequent wetting-drying cycles, indicating the gradual formation of a more interconnected crack network. In clay soil, CI increased from 0.210 in Cycle 1 to 0.233 in Cycle 5, while in silty clay it increased from 0.193 to 0.22 during the same time period. Tukey's multiple comparison test for cycles (Table 20) showed that Cycle 1 had far lower connectivity than Cycles 2-5, which were greater and statistically similar. This shows that after the first wetting-drying cycle, crack connectivity increased significantly and stabilized. This trend matches crack network physical evolution. Initial drying fractures are mainly discrete tensile fissures. These fractures reopen, proliferate, and merge with repeated wetting and drying, creating junctions and continuous passageways that promote connectivity. [19,22,23]revealed that cyclic drying progressively connects and stabilizes crack networks.

Table 21 shows how soil type affects crack connectedness. Clay had higher connectivity index (CI) values than silty clay across all wetting-drying cycles, indicating a tighter fracture network. In Cycle 1, clay showed a higher Tukey group (bc) than silty clay, with a CI of 0.210 ± 0.010 compared to 0.193 ± 0.006. This gap grew in successive rounds. In Cycles 4 and 5, clay showed the highest connection (0.233 ± 0.006 and 0.233 ± 0.012, group a), but silty clay remained in lower groups (0.210-0.220, abc-ab), indicating poorer network connectedness. Clay had more crack networks than silty clay after wetting-drying. Higher clay CI indicates higher clay mineral concentration and shrinks-swell potential, which increases drying tensile stresses and crack branching, intersection, and connecting. [18]found that clay-rich soils form more complex and well-connected fracture networks than silt-rich soils. Due to micro-crack propagation and fracture merging, clay-dominated soils exhibit denser and more integrated crack networks during cyclic wetting-drying, according to [19,23].

Table 19: Statistical significance of soil type, wetting–drying cycle, and their interaction on soil crack connectivity.

Term	P-Value	Interpretation
Soil Type	0.015	significant
Cycle	0.000	Highly significant
Soil Type*Cycle	0.363	Not significant

*Significant ($P < 0.05$), highly significant ($P < 0.001$) and not significant ($P > 0.05$).

Table 20: Tukey grouping of mean connectivity index across wetting–drying cycles (averaged over clay and silty clay soils).

Cycle	N	Mean
1	6	0.202 b
2	6	0.215 a
3	6	0.218 a
4	6	0.222 a
5	6	0.227 a

*Means that do not share a letter are significantly different (P < 0.05).

Table 21: Descriptive statistics (mean ± standard deviation) of mean connectivity index for clay and silty clay soils under successive wetting–drying cycles.

Cycle	clay soil	silty clay soil
1	0.210 ± 0.010 bc	0.193 ± 0.006 c
2	0.220 ± 0.010 ab	0.210 ± 0.010 abc
3	0.230 ± 0.000 ab	0.207 ± 0.006 bc
4	0.233 ± 0.006 a	0.210 ± 0.010 abc
5	0.233 ± 0.012 a	0.220 ± 0.000ab

*Means that do not share a letter are significantly different (P < 0.05).

Hydrological and Soil Management Implications

The observed evolution of soil crack characteristics under repeated wetting–drying cycles has important implications for soil hydrology. The marked decrease in crack number and crack area after the initial cycles, accompanied by a progressive increase in crack width and connectivity, indicates a transition from numerous isolated micro-cracks to fewer but more continuous preferential flow pathways. Such well-connected crack networks can significantly alter infiltration behavior by promoting rapid bypass flow during rainfall or irrigation events, thereby reducing matrix water retention and increasing spatial variability in soil moisture distribution. Previous studies have demonstrated that increased crack connectivity enhances preferential flow and accelerates solute transport in clay-rich soils, particularly under natural wetting conditions[14,22]. Therefore, the crack network maturation observed in this study suggests that repeated wetting–drying cycles can progressively intensify hydrological heterogeneity in clay and silty clay soils under field conditions.

From a soil management perspective, the stabilization of crack patterns after the third wetting–drying cycle highlights the critical role of early drying cycles in controlling soil structural evolution. The formation of wider and more connected cracks in clay soil compared to silty clay indicates a greater susceptibility of clay-rich soils to structural degradation and preferential flow development. These findings imply that management interventions aimed at reducing soil cracking—such as residue retention, organic amendments, surface mulching, or regulated irrigation scheduling—may be most effective when applied during the early stages of wetting–drying cycles. Similar management strategies have been reported to reduce crack severity, improve aggregate stability, and limit water loss in cracking-prone soils [19] . Consequently, understanding the temporal evolution of crack morphology provides a scientific basis for designing soil conservation and water management practices in semi-arid regions.

ISSN 2072-3857

Conclusions

This field-based study demonstrates that repeated wetting–drying cycles fundamentally reorganize crack systems in clay and silty clay soils, leading to the progressive stabilization of surface fracture networks. The results indicate that early wetting–drying cycles play a dominant role in determining long-term crack structure, while subsequent cycles primarily reinforce existing fracture pathways rather than creating new ones. From a soil hydrological perspective, the transition toward wider and more connected cracks suggests an increasing dominance of preferential flow, which can reduce soil water retention efficiency and promote uneven moisture redistribution during rainfall or irrigation events. These hydrological alterations are more pronounced in clay soils due to their higher shrink–swell potential, highlighting their greater vulnerability to water loss and rapid solute transport.

In terms of soil and irrigation management, the findings emphasize the importance of minimizing severe drying during the initial wetting–drying cycles. Management practices such as regulated irrigation scheduling, surface mulching, residue retention, and organic amendments may reduce crack connectivity and limit the development of persistent preferential flow pathways. Implementing such practices during early drying stages is likely to be more effective than corrective measures applied after crack networks have stabilized. Overall, understanding the temporal evolution of soil crack morphology provides a scientific basis for improving water-use efficiency, reducing structural degradation, and designing sustainable soil management strategies in semi-arid regions with cracking-prone soils.

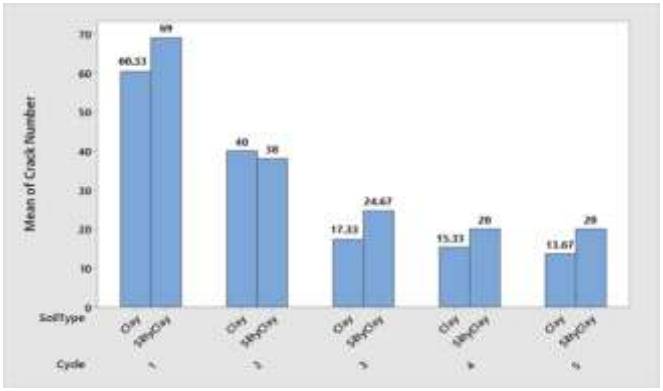

Figure 6: Variation of mean crack number with wetting–drying cycles in clay and silty clay soils.

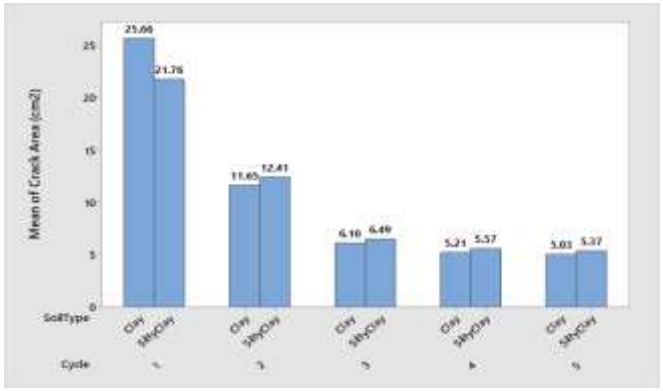

Figure 7: Variation of mean crack area with wetting–drying cycles in clay and silty clay

Figure 8: Variation of mean crack area (%) with wetting–drying cycles in clay and silty clay soils.

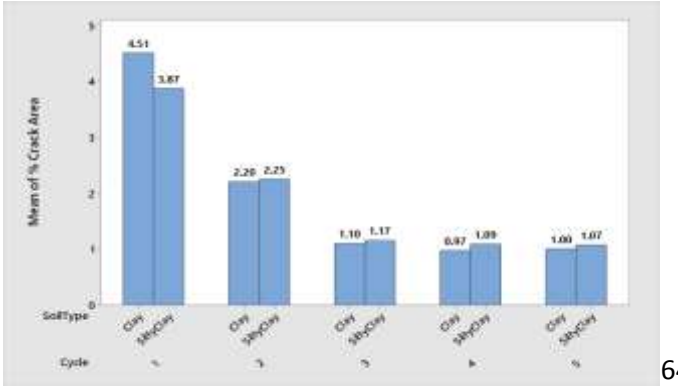

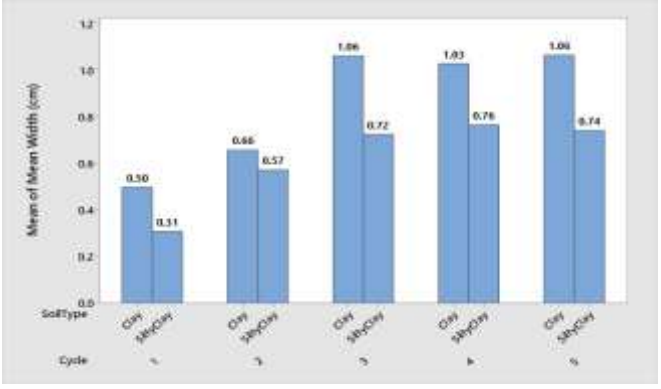

Figure 9: Variation of mean crack width with wetting–drying cycles in clay and silty clay soils.

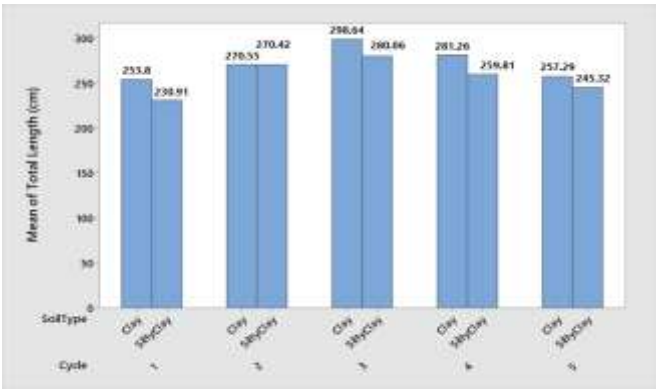

Figure 10: Variation of mean total crack length with wetting–drying cycles in clay and silty clay soils.

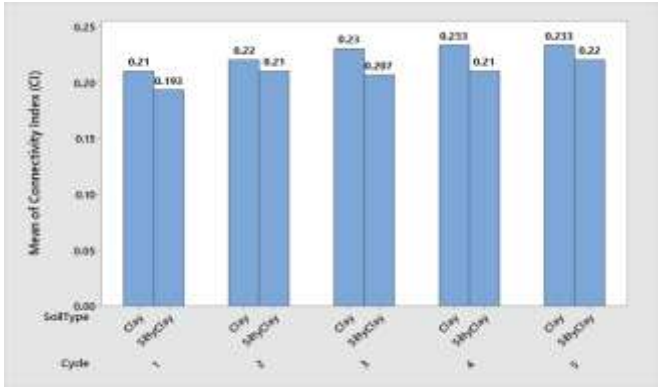

Figure 11: Variation of mean connectivity index with wetting–drying cycles in clay and silty clay soils.

Acknowledgment

The author gratefully acknowledges Prof. Akram Abbas Khalaf for his valuable supervision, constructive comments, and continuous academic support throughout this research. Appreciation is also extended to the Department of Soil and Water Sciences, College of Agriculture, for providing laboratory facilities and technical assistance necessary for conducting the experimental work. The author sincerely thanks all individuals who contributed directly or indirectly to the successful completion of this study.

References

1. Al Zubaydi, A. H. (2011). Effect of wetting and drying cycles on swell/collapse behavior and cracks of fine–grained soils. *Tikrit Journal of Engineering Sciences*, *18*(4), 71-79.
2. Al-Hiti, F. A., & Al-Nuaymy, W. S. S. (2023, December). Effect of accelerated physical weathering of coarse soils and wetting and drying cycle on some soil physical properties. In *IOP Conference Series: Earth and Environmental Science* (Vol. 1252, No. 1, p. 012051). IOP Publishing.
3. ASTM International. (2012). *Standard test methods for laboratory compaction characteristics of soil using standard effort* (ASTM D698-12e2). ASTM International. https://www.astm.org/Standards/D698.htm
4. ASTM International. (2014). *Standard test methods for specific gravity of soil solids by water pycnometer* (ASTM D854-14). ASTM International. https://www.astm.org/Standards/D854.htm
5. ASTM International. (2016). *Standard test method for determination of soil water characteristic curve for desorption using a hanging column, pressure extractor, or centrifuge* (ASTM D6836-16). ASTM International. https://www.astm.org/Standards/D6836.htm
6. ASTM International. (2016). *Standard test methods for laboratory determination of density (unit weight) of soil specimens* (ASTM

D7263-16). ASTM International. https://www.astm.org/Standards/D7263.htm
7. ASTM International. (2016). *Standard test methods for laboratory determination of water (moisture) content of soil and rock by mass* (ASTM D2216-16). ASTM International. https://www.astm.org/Standards/D2216.htm
8. ASTM International. (2017). *Standard test methods for liquid limit, plastic limit, and plasticity index of soils* (ASTM D4318-17e1). ASTM International. https://www.astm.org/Standards/D4318.htm
9. ASTM International. (2018). *Standard test methods for particle-size distribution (gradation) of fine-grained soils using the sedimentation (hydrometer) analysis* (ASTM D7928-17). ASTM International. https://www.astm.org/Standards/D7928.htm
10. Auvray, R., Rosin-Paumier, S., Abdallah, A., & Masrouri, F. (2014). Quantification of soft soil cracking during suction cycles by image processing. *European Journal of Environmental and Civil Engineering*, *18*(1), 11-32. v
11. Chen, X., Jing, X., Li, X., Chen, J., Ma, Q., & Liu, X. (2023). Slope crack propagation law and numerical simulation of expansive soil under Wetting–Drying cycles. *Sustainability*, *15*(7), 5655.
12. Hillel, D. (2004). *Introduction to environmental soil physics*. Elsevier Academic Press, Amsterdam.
13. Iraqi Meteorological and Seismology Organization. (2024). *Climatological data for Duhok station*. Baghdad, Iraq.
14. Luo, Y., Zhang, J., Zhou, Z., Aguilar-Lopez, J. P., Greco, R., & Bogaard, T. (2023). Effects of dynamic changes of desiccation cracks on preferential flow: experimental investigation and numerical modeling. *Hydrology and Earth System Sciences*, *27*(3), 783-808.
15. Qi, W., Wang, C., Zhang, Z., Huang, M., & Xu, J. (2022). Experimental investigation on the impact of drying–wetting cycles on the shrink–swell behavior of clay loam in farmland. *Agriculture*, *12*(2), 245.
16. Ralaizafisoloarivony, N., Degré, A., Mercatoris, B., Leonard, A., Toye, D., & Charlier, R. (2020, May). Assessing soil crack dynamics and water evaporation during dryings of agricultural soil from reduced tillage and conventional tillage fields. In *Proceedings* (Vol. 30, No. 1, p. 59). MDPI.
17. Schindelin, J., Arganda-Carreras, I., Frise, E., Kaynig, V., Longair, M., Pietzsch, T., Preibisch, S., Rueden, C., Saalfeld, S., Schmid, B., Tinevez, J.-Y., White, D. J., Hartenstein, V., Eliceiri, K., Tomancak, P., & Cardona, A. (2012). **Fiji: An open-source platform for biological-image analysis.** *Nature Methods*, *9*(7), 676–682.
18. Shafqat, K., Khalid, U., & Rehman, Z. U. (2025). Coupling effect of cyclic wet-dry environment and compaction state on desiccation cracking and mechanical behavior of low and high plastic clays. *Bulletin of Engineering Geology and the Environment*, *84*(2), 66.
19. Shaker, A. A., Dafalla, M., Al-Mahbashi, A. M., & Al-Shamrani, M. A. (2024). Effect of drying and wetting cycles on the surface cracking and hydro-mechanical behavior of expansive clays. *Buildings*, *14*(7), 1908.
20. Shit, P. K., Bhunia, G. S., & Maiti, R. (2015). Soil crack morphology analysis using image processing techniques. *Modeling Earth Systems and Environment*, *1*(4), 35.
21. Singh, S. P., Rout, S., & Tiwari, A. (2018). Quantification of desiccation cracks using image analysis technique. *International Journal of Geotechnical Engineering*, *12*(4), 383-388.
22. Tang, C. S., Cui, Y. J., Shi, B., Tang, A. M., & An, N. (2016). Effect of wetting-drying cycles on soil desiccation cracking behaviour. In *E3S Web of conferences* (Vol. 9, p. 12003). EDP Sciences.
23. Tu, Y., Zhang, R., Zhong, Z., & Chai, H. (2022). The Strength Behavior and Desiccation Crack Development of Silty Clay Subjected to Wetting–Drying Cycles. *Frontiers in earth science*, *10*, 852820.
24. Wan, Y., Xue, Q., Liu, L., & Wang, S. (2018). Crack Characteristic and Permeability Change of Compacted Clay Liners with Different Liquid Limits under Dry- Wet Cycles. *Advances in Civil Engineering*, *2018*(1), 5796086.

ISSN 2072-3857

25. Wei, X., Gao, C., & Liu, K. (2020). A review of cracking behavior and mechanism in clayey soils related to desiccation. *Advances in Civil Engineering*, *2020*(1), 8880873.

26. Zhao, Y., Zhang, H., Wang, G., Yang, Y., & Ouyang, M. (2024). Development Characteristics and Mechanism of Crack in Expansive Soil under Wet–Dry Cycling. *Applied Sciences*, *14*(15), 6499.

ISSN 2072-3857